X-ray analysis of the structure of the thermotropic copolyester poly(phenyl-*p*-phenylene terephthalate)

Sung-Kwon Hong and John Blackwell*
Department of Macromolecular Science, Case Western Reserve University, Cleveland, Ohio 44106-2699, USA
(Received 10 June 1988; revised 25 July 1988; accepted 29 July 1988)

X-ray methods have been used to determine the chain conformation and packing of the thermotropic copolyester prepared from terephthaloyl chloride (TPA) and phenylhydroquinone (PHQ). The X-ray patterns of annealed melt-spun fibres contain a series of sharp Bragg reflections, pointing to a well ordered crystalline structure, despite the random sense (2- or 3-) of the phenyl substituents on the TPA–hydroquinone backbone. The structure has been solved by linked-atom least-square methods. The unit cell is monoclinic with dimensions: $a=12.77$ Å, $b=10.08$ Å (unique axis) and $c=12.58$ Å (fibre axis); α, β and $\gamma=90°$. The space group is $P2_1$, and the cell contains TPA–PHQ units of four chains. The random phenyl substituents were modelled by placing these groups at both the 2- and 3-positions and giving each a weight of one-half. The final structure had $R=0.20$, after least-square refinement of nine parameters against 13 observed and 21 unobserved reflections. Packing of the side chains is effected by staggering adjacent chains along the b axis by approximately $c/2$, so that the side chains are interleaved. The phenyl–COO and COO–phenyl torsion angles are $-7.3°$ and 65.5°, with the result that the main-chain phenyls are mutually inclined at 58.2° (the ester groups are assumed to be planar). The phenyls of the phenyl hydroquinone units are mutually inclined at 59.3° (*ortho*) and 59.8° (*meta*). These torsion angles compare very well with those for model compounds, notably phenylbenzoate, and can be used in future analyses of the structure of more complex random-sequence copolyesters.

(Keywords: X-ray diffraction; polyesters; liquid-crystalline polymers; aromatic copolyesters; thermotropic polymers; structure determination; chain conformation)

INTRODUCTION

In this paper we describe X-ray analysis of the structure of a wholly aromatic polyester prepared from 50% terephthaloyl chloride (TPA) and 50% phenylhydroquinone (PHQ). This polyester[1] is a part of a family of aromatic thermotropic polyesters[2] that can be processed as self-reinforcing plastics or high-strength fibres[3]. The chemical structures and properties of these thermotropic polyesters have been reviewed by Jin *et al.*[4]. They generally contain aromatic units such as 1,4-phenylene, 4,4′-biphenylene and 2,6-naphthalenes, linked by ester groups. The melting points can be reduced by incorporation of side-chain substituents, main-chain 'kinks', such as 1,3-phenylene units, or flexible $(CH_2)_n$ spacers[5].

The X-ray diffraction patterns of annealed melt-spun fibres of this polyester show a high degree of orientation parallel to the fibre axis. The presence of sharp Bragg reflections on well defined layer lines indicates the existence of three-dimensional order[6], despite the random 2- and 3-substitution of the backbone hydroquinones. We have refined this structure by linked-atom least-square (LALS) methods[7], primarily in order to determine the chain conformation. This laboratory is engaged in a study of the structure of thermotropic copolyesters[8–15], notably the copolymer prepared from *p*-hydroxybenzoic acid (HBA) and 2-hydroxy-6-naphthoic acid. We have demonstrated that these are random copolymers based on the non-periodic layer lines observed in their fibre diagrams. In our most recent work[15] we have developed three-dimensional models for the ordered packing of these random copolymers, which presents us with the need for knowledge of the likely chain conformation.

EXPERIMENTAL

Synthesis

The polymer was synthesized from equimolar quantities of terephthaloyl chloride and phenylhydroquinone dissolved in methylene chloride in the presence of pyridine as an acid trap. Phenylhydroquinone and terephthaloyl chloride (reagent grades) were obtained from Eastman Kodak and Sigma Chemical Co., respectively. The reaction was conducted under a moderate nitrogen-flow blanket at approximately atmospheric pressure. The terephthaloyl chloride was added slowly to the phenylhydroquinone solution while stirring vigorously and maintaining the temperature at approximately 0°C. Upon completion of the polymerization, the solvent was extracted by distillation. The solid product was washed with water and acetone several times, filtered and dried in a vacuum oven at approximately 100°C and 500 mmHg overnight. The dried polymer had a melting point of ~350°C and inherent viscosity of ~0.45 dl g^{-1} when dissolved in

* To whom correspondence should be addressed

0032-3861/89/020225-06$03.00

equal volumes of trifluoroacetic acid and methylene chloride.

X-ray diffraction

Specimens for X-ray analysis were bundles of parallel fibres drawn by hand from the melt. These were examined both in the as-spun state and after they had been annealed at 250°C for 2 h. X-ray fibre diagrams were recorded on Kodak no-screen X-ray film using Ni-filtered Cu K_α radiation and a Searle toroidal focusing camera. The *d*-spacings were calibrated using calcium fluoride.

Intensity measurements

The integrated intensities of the observed reflections were determined using an Optronix Photoscan P1000 digital microdensitometer, as has been described elsewhere[16]. The data were recorded as an *x–y* scan of optical density and each reflection was integrated after subtraction of a local background determined as the averages from around its perimeter. Each *hkl* intensity was determined as the average of measurements and converted to $F^2(hkl)$ by application of Lorentz and polarization corrections (except for the 00*l* reflections). Unobserved reflections produced in the range of the observed data were assigned an intensity equal to half of the threshold for observation of a reflection in this region.

Molecular model building and refinement

Molecular models based on standard bond lengths and bond angles[17–19] were generated using the LALS program package. It was assumed that the phenyl groups are planar, and that the phenyl side chains are distributed equally between the *ortho*- and *meta*-positions. As will be seen below, the axial repeat for this polymer consists of a single TPA–PHQ unit, for which two models were considered for the positions of the phenyl substituents:

(1) 2-, 3-, 5- and 6-phenyls weighted by 0.25, allowing for random *o*- and *m*-substitution on both sides of the chain; and

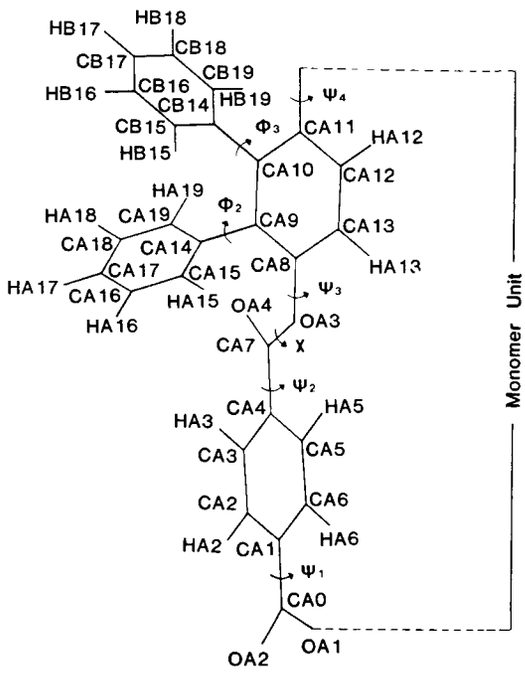

Figure 1 Numbering of the atoms and definition of the refinable torsion angles for the polymer repeat unit (model 2)

(2) 2- and 3-phenyls, requiring the substituents to be always on the same side of the chain.

The refinable parameters in case 2 are shown in *Figure 1*. The phenyl groups are assumed to be planar. All torsion angles are defined as positive for anticlockwise rotations, and 0° corresponds to the *cis* conformation in each case. The ester groups are assumed to be planar ($\chi=0°$). The conformation is defined by two backbone torsion angles, $\psi_2(=\psi_1)$ and $\psi_3(=\psi_4)$, i.e. the phenyl–ester inclinations, and the side-chain phenyl torsion angles, ϕ_2 and ϕ_3. For model 1, two additional side-chain torsion angles, ϕ_5 and ϕ_6 are necessary. The unit cell contains four chains, but these form two pairs of two chains related by a 2_1 screw axis along the *b* axis. The axial rotations of the independent chains passing through 0,0 and $\frac{1}{2}$,0 on the *ab* face are θ_1 and θ_2, and s_1 and s_2 are the shifts for their ester oxygens (OA1) along the *c* axis, respectively. In the last stages of the refinement we considered the possibility of the small shifts of the chain axis along the *a* and *b* axes, away from the 0,0 and $\frac{1}{2}$,0 positions. These shifts are s_3, s_4 for the 0,0 chain and s_5, s_6 for the $\frac{1}{2}$,0 chain respectively. The remaining parameters are *K*, the scale factor to put the observed structure amplitudes on the same scale as those calculated, and *B*, an isotropic temperature factor.

These parameters are varied in the LALS procedure so as to minimize the function:

$$\phi=\sum_i W_i(|{}_oF_i|-|{}_cF_i|)^2+\sum_L A_L G_L+\sum\varepsilon_{ij} \qquad (1)$$

where ${}_oF_i$ and ${}_cF_i$ are the observed and calculated structure amplitudes for the *i*th reflection and W_i is an assigned weight: in the present work, we used $w=1$ for observed and $w=\frac{1}{2}$ for unobserved reflections. A_L are Lagrange multipliers assigned to functions G_L that define stereochemical constraints applied to the structure. These constraints arise principally from the requirement of helical symmetry. The third summation covers all variable non-bonded interatomic distances d_{ij} less than a specified minimum ${}_od_{ij}$:

$$\begin{aligned} \varepsilon_{ij}&=K_{ij}({}_od_{ij}-d_{ij}) \qquad & d_{ij}<{}_od_{ij} \\ \varepsilon_{ij}&=0 & d_{ij}\geqslant {}_od_{ij} \end{aligned} \qquad (2)$$

The values of K_{ij} were based on the potential energy calculations of Chandrasekaran and Balasubramanian[20], as used by Arnott and Smith[7]. Each ${}_od_{ij}$ was set at 0.2 Å greater than the sum of van der Waals radii, to ensure that all short contacts were driven to larger values.

RESULTS AND DISCUSSION

Unit-cell determination

The X-ray fibre diffraction patterns of as-spun and annealed samples are shown in *Figure 2*. Annealing leads to the development of sharp Bragg reflections, pointing to an ordered three-dimensional structure for the copolymer. The present paper analyses the structure of the annealed state: the as-spun state, which appears to be the same as in unoriented powder, will be considered at a later date.

The unit-cell dimensions and other crystal data are shown in *Table 1*. The unit cell was determined by trial and error followed by least-square refinement, based on

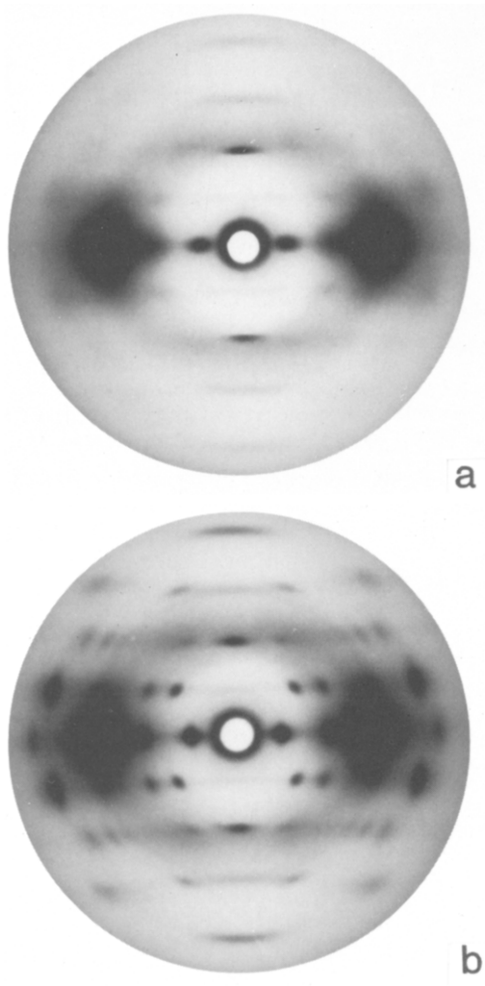

Figure 2 X-ray diffraction patterns for melt-spun fibres of poly(phenyl-*p*-phenylene terephthalate): (a) as-spun; (b) annealed at 250°C for 2 h

Table 1 Crystal data[a]

a (Å)	12.77 (0.08)
b (Å)	10.08 (0.07)
c (Å)	12.58 (0.07)
Volume (Å^3)	1619.3
Density (g cm^{-3})	1.313
Measured density (g cm^{-3})	1.300
No. of chain (*Z*)	4
Space group	$P2_1$

[a] Standard deviations in parentheses

the *d*-spacings of 16 observed reflections with $d > 3$ Å. The unit cell has dimensions: $a = 12.77(0.08)$ Å, $b = 10.08(0.07)$ Å and *c* (chain axis) $= 12.58(0.07)$ Å, with monoclinic geometry (α, β and $\gamma = 90°$). The observed and calculated *d*-spacings are shown in *Table 2*, and for most reflections the agreement is within 1%. The most obvious discrepancies are for the 200 reflection (1.7%) and the 020 reflection (1.9%). In view of the random substitution of the phenyl groups, the X-ray data yield only an average unit cell, and the actual packing will vary for the different substituent positions on adjacent chains. The distortions inherent in such a structure probably account for the less than perfect agreement between the observed and calculated *d*-spacings. The only systematic absences are for the odd-order $0k0$ reflections, pointing to a monoclinic $P2_1$ space group, with the unique axis parallel to *b*.

The fibre diagram shows a series of periodic layer lines with spacing $c = 12.58$ Å, which is comparable to the repeat of 12.9 Å for poly(*p*-phenylene terephthalamide)[21] and 12.6 Å for poly(oxybenzoate)[22]. Thus we expect that the copolymer has an analogous extended conformation, with *c* corresponding to the length of a single PHQ–TPA unit. The unit cell has a volume of 1619 Å^3: if this contains four PHQ–TPA units, the calculated density is 1.313 g cm^{-3}, which agrees very well with the observed density of 1.30 g cm^{-3} determined by flotation.

Refinement of the structure

Independent chains were positioned with their axes passing through (0,0) and ($\frac{1}{2}$,0) in the *ab* plane. The 2_1 screw axis generates two more chains through (0,$\frac{1}{2}$) and ($\frac{1}{2}$,$\frac{1}{2}$). In the initial refinement we used model 1 for the chain, with phenyls weighted 0.25 at the 2-, 3-, 5- and 6-positions on the hydroquinone. We refined 12 parameters: $s_1, s_2, \psi_2, \psi_3, \theta_1, \theta_2, \phi_2, \phi_3, \phi_5, \phi_6, K$ and *B*, first in groups and then altogether, to obtain the best agreement between the observed and calculated structure amplitudes. The best *R* value obtained was 0.24, but the structures were stereochemically unacceptable because of many side chain–side chain bad contacts. Introduction of constraints to reduce the bad contacts resulted in some improvement, but the *R* value increased to the mid 30s, and some bad contacts still remained, even when shifts of the chains along the *a* and *b* axes were allowed. Examination of the models shows that bad contacts are unavoidable in a structure in which the phenyl side chains are randomly disposed on both sides of the TPA–PHQ repeat.

When we used model 2 for the chain conformation, in which the phenyls are at the 2- and 3-positions and weighted by 0.5, we obtained considerable improvement. The *R* values fell immediately to the mid 20s, and the final refined value was 0.20. When possible shifts of the chain axes along the *a* and *b* axes were considered these were found to be negligible. The torsion angles and atomic coordinates for the refined structure are given in *Tables 3* and *4*, and the observed and calculated structure amplitudes are compared in *Table 5*. The *ab* projection of the unit cell is shown in *Figure 3*. The packing of the side chain is illustrated in *Figure 4*, which shows projections of two chains on (a) the 020 and (b) the 200 plane.

Table 2 Comparison of observed and calculated *d*-spacings

hkl	d_{calc} (Å)	d_{obs} (Å)
100	12.77	12.63
200	6.38	6.28
020	5.04	4.95
120	4.69	4.66
410	3.04	3.07
011	7.86	7.75
201	5.69	5.79
121	4.03	4.08
031	3.25	3.29
002	6.29	6.26
102	5.64	5.59
022	3.76	3.77
302	3.52	3.46
013	3.87	3.89
123	3.13	3.11
004	3.05	3.07

The final structure has adjacent chains along the a axis with their ester oxygens staggered by $0.032c$ and their phenyl substituents disposed to opposite sides of the chain. The 2_1 screw axis parallel to b has the effect that for the chains in that direction the phenyls are also disposed to opposite sides. The side chains on chains along the ab diagonal point towards one another, but are interleaved since there is an effective stagger of $c/2$ between chains along the b axis.

The refined structure has a number of bad contacts, all of which are between the side groups of adjacent chains.

Table 3 Refined torsion angles

	Angle (deg)
O_A1–C_A0–C_A1–C_A2	−174.7
C_A3–C_A4–C_A7–O_A3	172.7
C_A3–C_A4–C_A7–O_A4	−7.3
C_A7–O_A3–C_A8–C_A9	65.5
C_A8–C_A9–C_A14–C_A15(*ortho*)	59.3
C_A9–C_A10–C_A14–C_A15(*meta*)	59.8

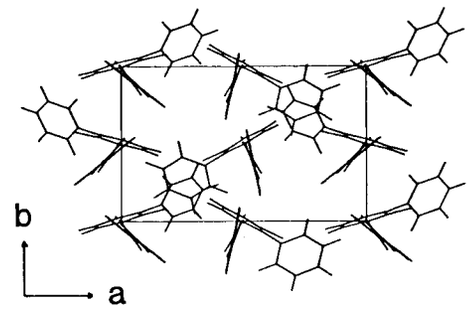

Figure 3 Projection of the refined structure on the ab plane

Table 4 Fractional atomic coordinates[a]

Atom	x	y	z	Atom	x	y	z
Chain at 0,0							
O_A1	−0.011	0.024	0.029	(*ortho*)C_A14	0.181	0.078	0.679
C_A0	0.056	−0.072	0.061	C_A15	0.191	0.177	0.603
O_A2	0.106	−0.142	0.003	H_A15	0.124	0.235	0.581
C_A1	0.057	−0.077	0.179	C_A16	0.287	0.202	0.555
C_A2	0.128	−0.162	0.228	H_A16	0.294	0.278	0.497
H_A2	0.176	−0.220	0.183	C_A17	0.374	0.127	0.584
C_A3	0.131	−0.169	0.338	H_A17	0.448	0.146	0.547
H_A3	0.185	−0.234	0.376	C_A18	0.364	0.028	0.659
C_A4	0.065	−0.091	0.399	H_A18	0.431	−0.030	0.681
C_A5	−0.005	−0.006	0.350	C_A19	0.269	−0.004	0.707
H_A5	−0.005	0.053	0.396	H_A19	0.260	−0.073	0.766
C_A6	−0.009	0.001	0.240	(*meta*)C_A14	0.162	0.102	0.906
H_A6	−0.063	0.067	0.202	C_B15	0.250	0.023	0.906
C_A7	0.065	−0.093	0.517	H_B15	0.251	−0.062	0.860
O_A3	0.002	0.005	0.557	C_B16	0.336	0.058	0.968
O_A4	0.112	−0.169	0.572	H_B16	0.401	0.001	0.968
C_A8	−0.007	0.017	0.669	C_B17	0.330	0.172	1.030
C_A9	0.078	0.052	0.730	H_B17	0.393	0.195	1.075
C_A10	0.067	0.063	0.840	C_B18	0.240	0.248	1.030
C_A11	−0.028	0.039	0.897	H_A18	0.238	0.334	1.076
C_A12	−0.114	0.003	0.836	C_B19	0.156	0.215	0.968
H_A12	−0.182	−0.014	0.859	H_B19	0.089	0.273	0.968
C_A13	−0.103	−0.008	0.716	O_A5	−0.024	0.039	1.009
H_A13	−0.170	−0.035	0.669				
Chain at $\frac{1}{2}$,0							
O_A1	0.490	0.031	−0.003	(*ortho*)C_A14	0.597	−0.181	0.647
C_AO	0.442	−0.082	0.029	C_A15	0.673	−0.158	0.571
O_A2	0.407	−0.165	−0.029	H_A15	0.693	−0.059	0.549
C_A1	0.439	−0.085	0.147	C_A16	0.724	−0.264	0.523
C_A2	0.400	−0.198	0.196	H_A16	0.784	−0.247	0.464
H_A2	0.374	−0.276	0.151	C_A17	0.699	−0.393	0.551
C_A3	0.396	−0.205	0.306	H_A17	0.738	−0.475	0.515
H_A3	0.366	−0.291	0.343	C_A18	0.622	−0.416	0.649
C_A4	0.431	−0.099	0.367	H_A18	0.602	−0.515	0.649
C_A5	0.470	0.013	0.318	C_A19	0.571	−0.310	0.675
H_A5	0.497	0.092	0.404	H_A19	0.510	−0.327	0.734
C_A6	0.474	0.020	0.208	(*meta*)C_B14	0.606	−0.147	0.874
H_A6	0.505	0.106	0.170	C_B15	0.579	−0.279	0.874
C_A7	0.429	−0.100	0.485	H_B15	0.517	−0.311	0.828
O_A3	0.479	0.008	0.525	C_B16	0.634	−0.369	0.936
O_A4	0.389	−0.182	0.540	H_B16	0.614	−0.468	0.936
C_A8	0.486	0.024	0.637	C_B17	0.717	−0.325	0.998
C_A9	0.542	−0.066	0.698	H_B17	0.759	−0.392	1.043
C_A10	0.546	−0.049	0.808	C_B18	0.745	−0.192	0.998
C_A11	0.496	0.056	0.865	H_B18	0.807	−0.160	1.044
C_A12	0.440	0.146	0.794	C_B19	0.689	−0.102	0.936
H_A12	0.404	0.221	0.827	H_B19	0.710	−0.004	0.936
C_A13	0.436	0.129	0.684	O_A5	0.499	0.049	0.977
H_A13	0.393	0.199	0.637				

[a] The chains at $0,\frac{1}{2}$ and $\frac{1}{2},\frac{1}{2}$ are related to those at 0,0 and $\frac{1}{2}$,0, respectively, by the 2_1 symmetry operation along the b axis: $-x, y+0.5, 1-z$ and $1-z, y+0.5, 1-z$

Table 5 Observed and calculated structure factors

hkl	F_{obs}	F_{calc}	hkl	F_{obs}	F_{calc}
100	299.9	134.6	021	40.8	66.6
200	332.4	352.1	023	75.3	80.7
410	270.1	287.7	101	40.8	38.8
011	111.6	105.6	012	13.6	11.9
201	104.5	88.5	113	40.8	38.8
121	211.5	208.4	111	13.6	8.4
031	220.8	214.2	112	54.5	87.9
301	204.2	196.1	122	40.8	59.4
221	95.3	99.2	202	27.2	19.2
311	94.5	78.8	211	13.6	10.3
102	98.1	65.1	212	27.2	37.2
022	109.1	80.7	320	27.2	39.2
302	98.9	87.5	303	71.7	79.7
032	75.3	98.5	123	177.8	141.8
013	124.9	89.3	203	85.3	112.9
103	56.3	55.8	213	56.3	58.2

However, there are less of these than when we use model 1. Of course, some bad contacts are inevitable since we are trying to pack molecules with two rather than one phenyl side chain per repeat. The contact situation is improved by the introduction of constraints but not eliminated. Since there are two possible positions for each side chain then each bad contact occurs for only 25% of the possible side chain–side chain combinations, and there is space corresponding to the other possible side-chain positions which allows for torsional rotation of the phenyls so as to eliminate the bad contacts. We have refined an average structure and have assumed that the ϕ_2 and ϕ_3 are independent of the position of its neighbour, whereas the actual angles will depend on the local environment.

The backbone chain conformation is defined by ψ_2 and ψ_3, the COO–phenyl and phenyl–COO torsion angles, which are $-7.3°$ and 65.5°, respectively. These compare very well with the observed values of $-9.8°$ and 65.1° reported for phenylbenzoate[23]. Survey of other model compounds shows ranges of $-3°$ to $-10°$ and 60° to 70° for the same two angles[24–27]. An *ab initio* quantum-chemistry calculation of the minimum energy conformation for an isolated phenylbenzoate molecule resulted in values of $-3.7°$ and 61.9° for the same angles, with $\chi = 0.6°$ (deviation from planarity of the ester group)[28]. The mutual inclination of the main-chain phenyls is 58.2°, compared to 55.7° in phenylbenzoate and a general observed range of 60–70°, including 68° in poly(*p*-phenylene terephthalamide)[21]. In the latter structure, the backbone torsion angles are 38° and $-30°$, but the linkages are via amide rather than ester groups, and it is also necessary to form intramolecular hydrogen bonds. The phenyl side chains in poly(TPA–PHQ) are inclined at 59.3° (*ortho*) and 59.8° (*meta*) to the main-chain phenyl of the PHQ moiety, very much consistent with the inclinations of 56.2° and 50.8° for the phenyl rings in 6,7-diphenyl[1,2,4]triazolo[5,1-*c*][1,2,4]-triazine[29].

We have refined this structure in part to provide conformational data for other random copolyesters, for which chemical sequence is more complex and X-ray data are more diffuse. The similarity of the refined conformation to those for model compounds gives us confidence to transfer them to other structures. Indeed it is very interesting that the X-ray data are so sensitive to these torsion angles. The intensities must be determined largely by the mutual inclination of the phenyl groups, and many combinations of ψ_2 and ψ_3 are possible that are compatible with a mutual inclination of 60° for the backbone phenyls. The high degree of crystalline order is perhaps surprising given the random substitution of the phenyl side chains. There must be differences in local packing of these groups, depending on the actual substitution, but these distortions do not prevent refinement of an average structure. We are currently working on the structure of the related copolymer in which the hydroquinone substituents are 50% phenyl and 50% 1-phenylethyl groups, and this work will be reported shortly.

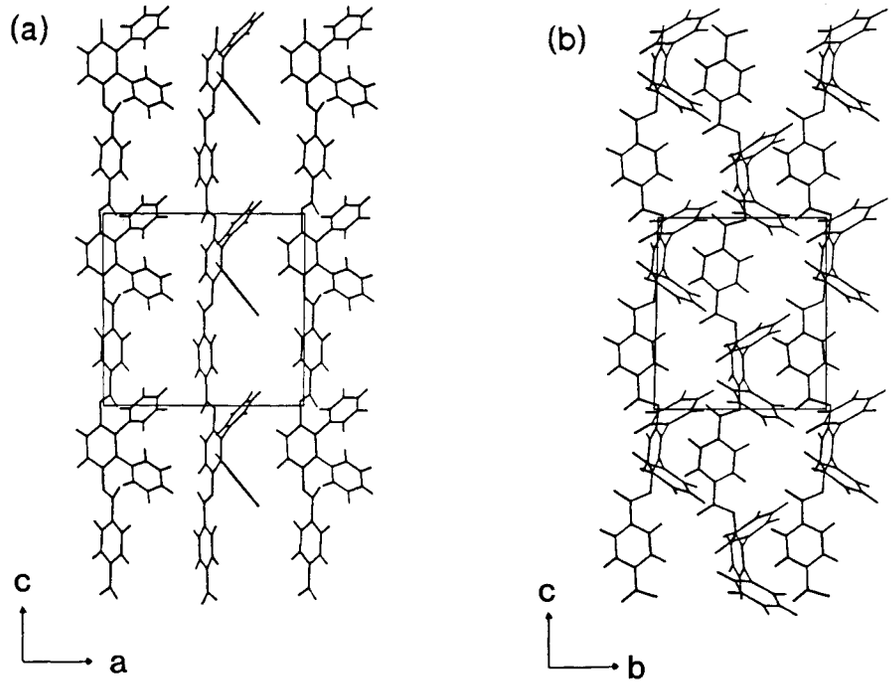

Figure 4 (a) Projection of two chains on the *ac* plane (020). (b) Projection of two chains on the *bc* plane (200)

ACKNOWLEDGEMENTS

We thank Professor Virgil Percec for his advice and assistance in the synthesis of the polymer. This work has been supported by NSF Grant No. DMR 84-17525 from the polymer programme.

REFERENCES

1 Payet, C. R. US Patent 4159365, 1979
2 Jackson, W. J. *Br. Polym. J.* 1980, **12**, 154
3 Dobb, M. G. and McIntyre, J. E. *Adv. Polym. Sci.* 1984, **60/61**, 61
4 Jin, J. I., Antoun, S., Ober, C. and Lenz, R. W. *Br. Polym. J.* 1980, **12**, 132
5 Kuhfuss, H. F. and Jackson, W. J. *J. Polym. Sci., Polym. Chem. Edn.* 1976, **14**, 2043
6 Stamatoff, J. B. *Mol. Cryst. Liq. Cryst.* 1984, **110**, 75
7 Smith, C. and Arnott, S. *Acta Crystallogr.* (*A*) 1978, **34**, 3
8 Blackwell, J. and Gutierrez, G. A. *Polymer* 1982, **23**, 671
9 Blackwell, J., Gutierrez, G. A., Chivers, R. A., Stamatoff, J. B. and Yoon, H. *Polymer* 1983, **24**, 937
10 Blackwell, J., Gutierrez, G. A. and Chivers, R. A. *Macromolecules* 1984, **17**, 1219
11 Blackwell, J., Gutierrez, G. A., Chivers, R. A. and Ruland, W. *J. Polym. Sci., Polym. Phys. Edn.* 1984, **22**, 1343
12 Blackwell, J., Biswas, A. and Bonart, R. C. *Macromolecules* 1985, **18**, 2126
13 Blackwell, J., Gutierrez, G. A. and Chivers, R. A. *Polymer* 1985, **26**, 348
14 Blackwell, J., Cheng, H. M. and Biswas, A. *Macromolecules* 1988, **21**, 39
15 Blackwell, J. and Biswas, A. *Macromolecules* in press
16 Hall, I. H. and Pass, M. G. *J. Appl. Crystallogr.* 1975, 60
17 Bailey, M. and Brown, C. J. *Acta Crystallogr.* 1967, **22**, 387
18 Anderson, K. E. *Acta Crystallogr.* 1967, **22**, 188
19 Hargreaves, A. and Hasan, R. S. *Acta Crystallogr.* 1962, **15**, 365
20 Chandrasekaran, R. and Balasubramanian, R. *Biochim. Biophys. Acta* 1969, **188**, 1
21 Northolt, M. G. *Eur. Polym. J.* 1974, **10**, 799
22 Blackwell, J., Lieser, G. and Gutierrez, G. A. *Macromolecules* 1983, **16**, 1418
23 Adams, J. M. and Morsi, S. E. *Acta Crystallogr.* (*B*) 1976, **32**, 1345
24 Brisse, F. and Perez, S. *Acta Crystallogr.* (*B*) 1976, **32**, 2110
25 Desborough, I. J., Hall, I. J. and Neisser, J. Z. *Polymer* 1979, **20**, 545
26 Colapietro, M. and Domenicano, A. *Acta Crystallogr.* (*B*) 1978, **34**, 3277
27 Perez, S. and Brisse, F. *Acta Crystallogr.* (*B*) 1976, **32**, 470
28 Jaffe, R. and Yoon, D., private communication, 1988
29 Schwalbe, C. H. *et al. Acta Crystallogr.* (*B*) 1978, **34**, 3409